



RECENT ADVANCES ON DROPS EVAPORATION ON STRUCTURED SUBSTRATES, CRYSTALLIZATION AND INDUCED MOTION

K. Sefiane*, Y. Chen¹ H. Zhao¹ M. Efstratiou, V. Kubyshkina, J. Christy, D. Orejon

¹School of Engineering, Institute for Multiscale Thermofluids, James Clerk Maxwell Building | Peter Guthrie Tait Road, EH9 3FD, Scotland, United Kingdom

1. ABSTRACT

This lecture will focus on some recent experimental advances on the evaporation of sessile droplets. The lecture will present results on the evaporation of droplets on viscoelastic substrates, crystallization during the evaporation of saline droplets, evaporation of nanofluid drops on structured surfaces and controlling motion of droplets on designed striated substrates and thermocapillary motion of drops on temperature gradients.

2. VISCOELASTIC SUBSTRATES

Drop evaporation on soft materials exists extensively in daily life and industrial applications, such as thermoregulation of human body, spray cooling, microfluidic devices, etc. However, this topic has not yet been understood as clearly as that on rigid substrates. In the present work, we investigate the evaporation of both pure water and nano suspension sessile drops on viscoelastic polydimethylsiloxane (PDMS) films. The viscoelasticity of PDMS surfaces was varied by controlling curing ratio and categorised into three types: stiff (10:1, 20:1, 40:1), relatively soft (60:1, 80:1) and very soft ones (100:1, 120:1, 140:1, 160:1).

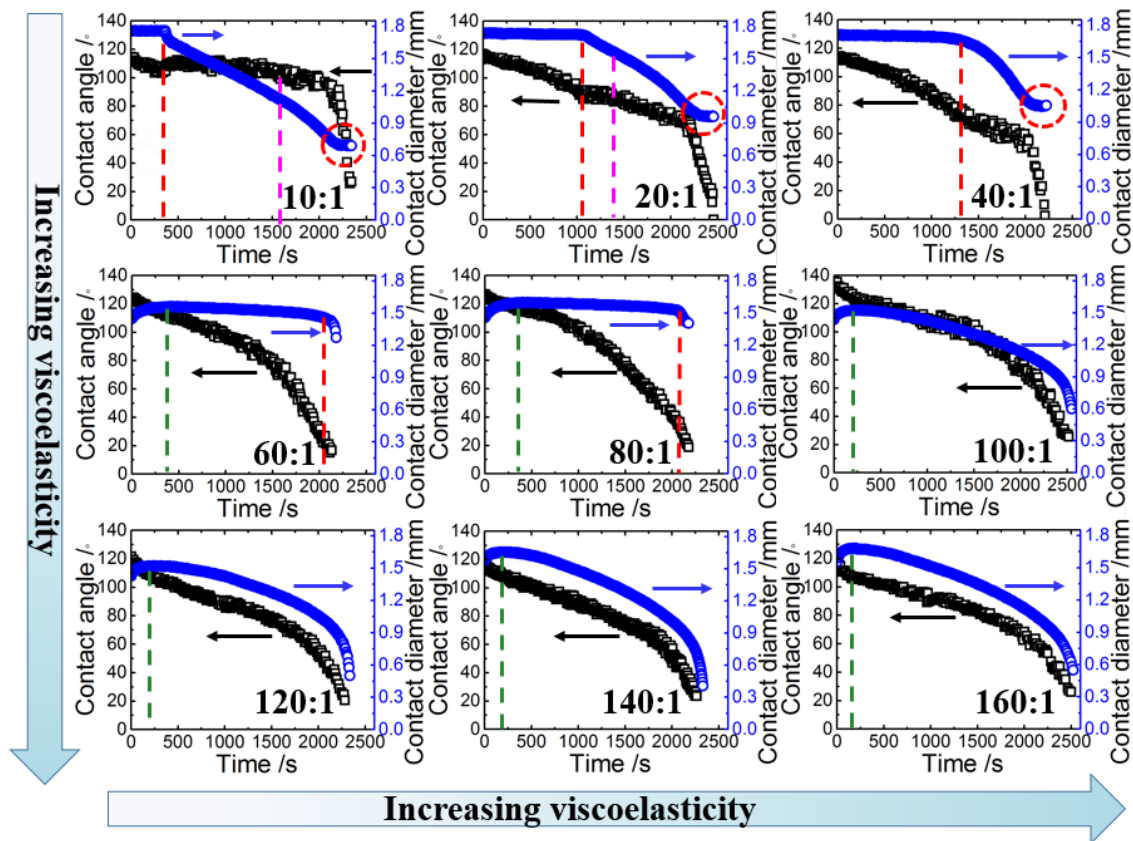


Figure 1: The temporal evolution of contact angle and contact diameter of nano suspension drops evaporating on various viscoelastic surfaces. The red, magenta and green dashed lines mark the CCR, CCA and spreading modes, respectively. Red circles mark the second CCR stage on stiff substrates.

We found that a water drop initially evaporates on stiff surfaces with a constant contact radius (CCR), followed by a constant contact angle (CCA) mode and a mixed mode. In contrast, nano suspension drops follow the same trend as pure water drops with a difference towards the end of their lifetime where a short second CCR mode is observed. On relatively soft surfaces, pure water and nano suspension drops initially spread then followed by a pseudo-CCR evaporation mode. On very soft substrates, the spreading is unexpectedly followed by a mixed mode, which is attributed to the horizontal displacement of the wetting ridge formed in the vicinity of the contact line. Like surface defects, the wetting ridge has the contact line anchored therein. As evaporation goes further, contact angle decreases and breaks the force balance at the contact line. The resulting net force in horizontal direction is transferred to and drags the wetting ridge to move with respect to the bulk of the substrate underneath, Figure 1. As a result, the contact line seemingly retreats at the same time and the mixed evaporation mode occurs. Thanks to the wide range of the viscoelasticity of substrates studied, we get an overall insight into its influence on the evaporation kinetics of sessile drop, especially relating the dynamics of wetting ridge to contact line behaviour [1].

3. CRYSTALLISATION-DRIVEN FLOWS IN DRYING AQUEOUS SALINE MICROLITER DROPLETS

The evaporative behaviour of aqueous saline droplets has been the subject of interest of many studies. Researchers have focused either on the investigation of the final desiccation patterns¹⁻⁴ or on the flow visualisation during drying⁵⁻⁷. However, no work has shown the interplay between the flows and salt crystallisation during evaporation. Our work shows the direct correlation between hydrodynamics and salt crystallisation within aqueous saline (1M) microliter droplets ($1.2 \pm 0.2 \mu\text{L}$), drying on hydrophilic glass slides. Micro-PIV (Particle Image Velocimetry) was employed for flow visualisation and

measurement of the velocities at the flat base of the drops. Two evaporation stages were exhibited; we refer to these as Stages I and II. During the early part of Stage I a generally outward flow manifests, similar to that observed in the case of evaporating pure water droplets. Measured velocities at the base of the drop range between 1-3 $\mu\text{m/s}$. This stage continues until $\sim 60\%$ of the droplet lifetime. During late stage I a subsequent “pause” of the flow is observed, lasting up to $\sim 70\%$ of the droplet lifetime. During this stage the flow velocities at the base of the drop decrease by orders of magnitude immediately before the nucleation of the first crystal on the periphery of the drop. Stage II is the most important stage, showing that crystallisation has a direct impact on the flow regime by inducing strong jets of fluid, directed towards the point of crystal nucleation and growth. The maximum velocity in the jet is $\sim 20\mu\text{m/s}$. The jets of fluid lead to increasing vorticity on either side of the growing crystals where the concentration decreases, providing a potential explanation as to why NaCl deposits as a ring of spaced crystals, rather than the classical continuous “coffee-ring” reported by Deegan⁸. Calculations of the base velocities were carried out for each evaporation stage considering both continuity and solutal Marangoni convection acting during crystal nucleation and growth. The calculated velocities are in good agreement with the measured experimental flow velocities, revealing that both continuity and solutal Marangoni convection affect the flow regime because of salt concentration changes. IRT was also utilised to rule out that the observed flows are due to thermal effects. Images of the drying drop at different evaporation stages and of the final desiccation deposit are shown in Figure 2, [2].

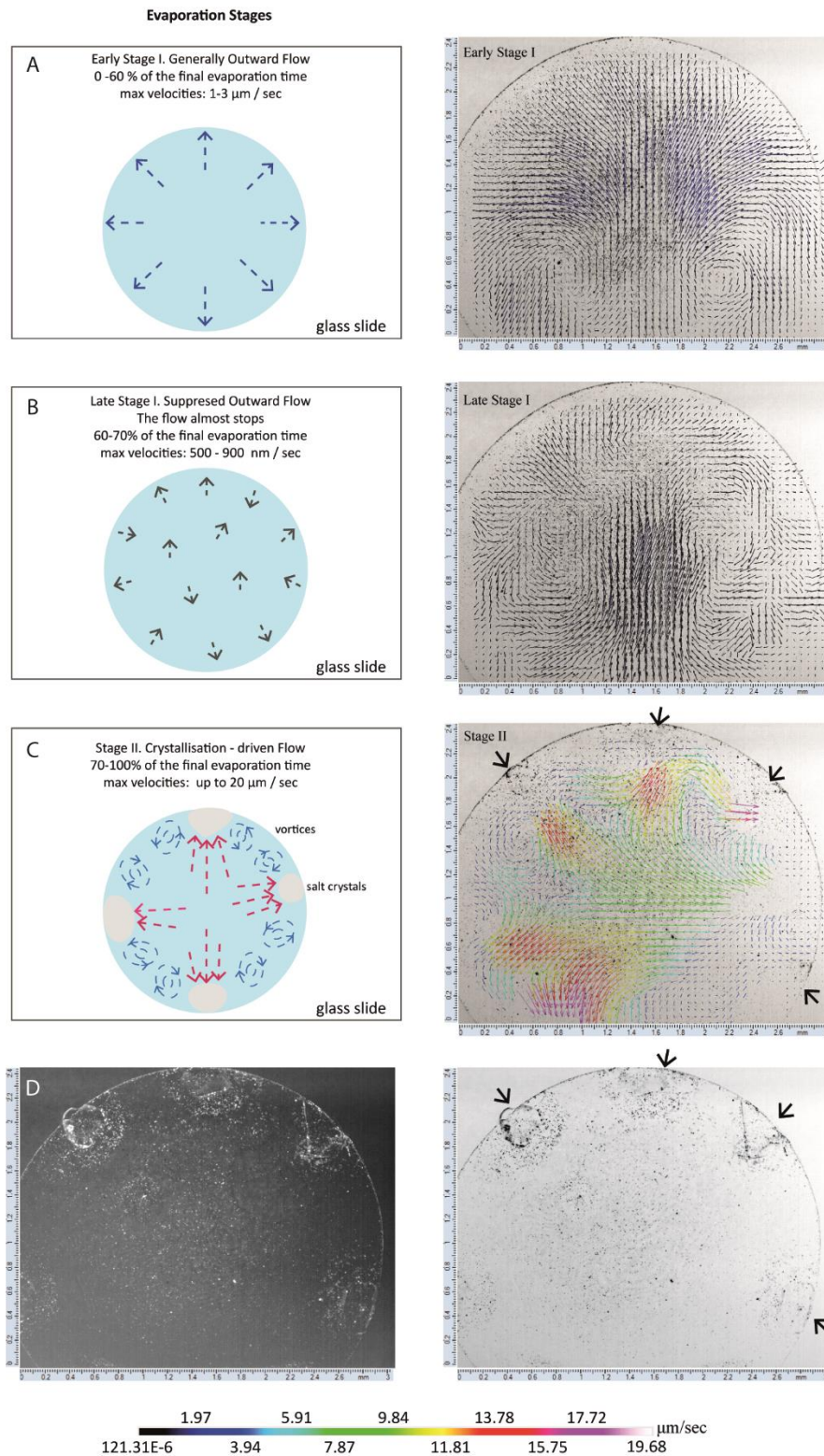


Figure 2: Evaporation stages and the final dried deposit of aqueous saline (1M) microliter drops on hydrophilic glass slides. A, B, and C show the evaporation stages (Early stage I, late stage I and stage II respectively). The left column shows schematics describing the evaporation stage, whereas the right column shows the velocity vectors acquired via micro-PIV. A and B show early and late stage I characterised by an outward flow and a “pause” of the flow respectively. C shows the strong jets of flow towards the growing crystals in stage II. D shows the final dried deposit as acquired by micro-PIV (left) and with inverted colours (right).

4. EVAPORATION OF NANOFLUID DROPLETS ON STRUCTURED SURFACES

Driven by growing applications involving drops interaction with solids and undergoing phase change, the topic of evaporation and drying of drops on textured surfaces has been subject to extensive recent research. In this part we present the results combining the evaporation of sessile droplets laden with nanoparticles and/on textured surfaces. The results demonstrate that the size, shape and spacing of textures dictate the initial shape of both pure and nanofluid drops. Circular, square, rectangular as well hexagonal shapes are observed correspondingly. The drying of nanofluid drops on these textured surfaces are studied to elucidate the deposition of nanoparticles and how they are affected by the textures and the initial shape. Particles deposition following dryout is found to be enhanced near the corners where curvature is greatest. Furthermore at a high nanofluid concentration, we observe self-assembly of particles into highly ordered intricate structures, Figure 3 and Figure 4.

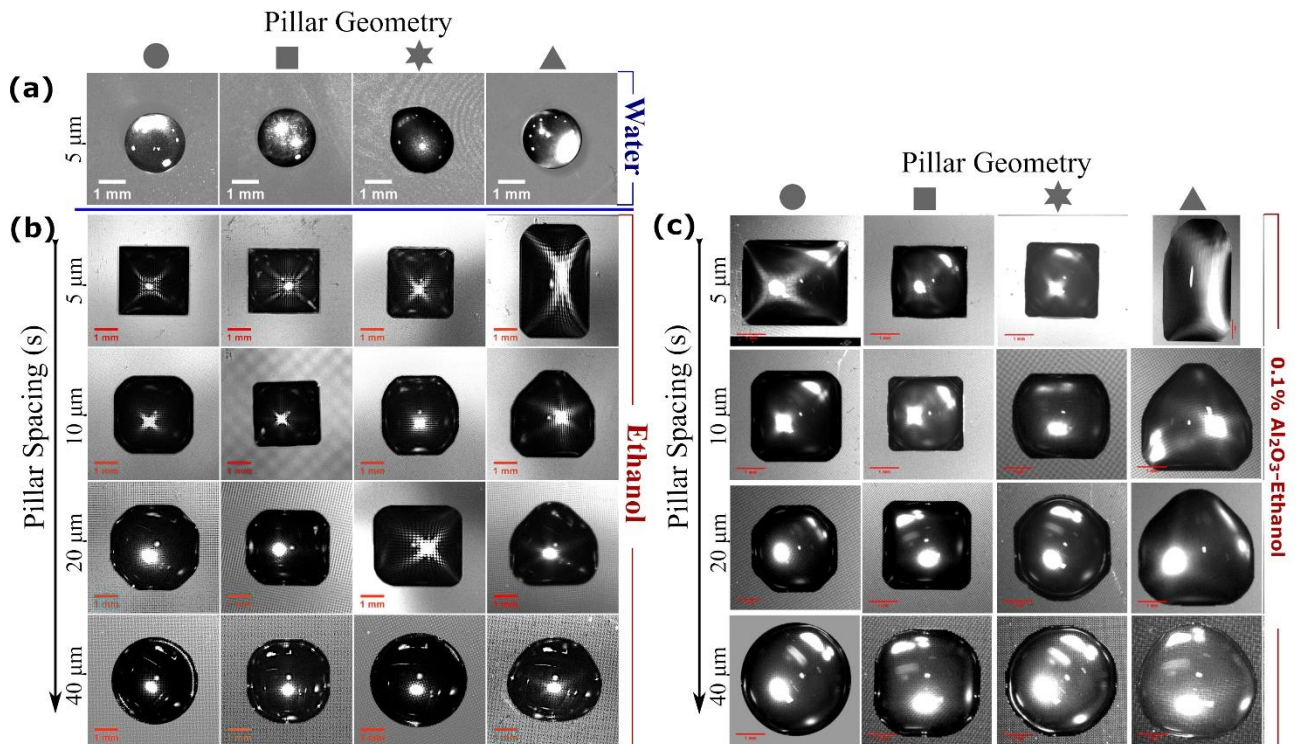


Figure 3: Snapshots looking from the top of the initial droplet wetting profile on substrates with circular, square, star and triangular shaped pillars (left to right). Scale bar is 1 mm for (a) pure water droplets on substrates with different pillar geometries, all with a spacing of 5 μm; (b) pure ethanol and (c) 0.1% Al₂O₃-ethanol nanofluid droplets on substrates with

different pillar geometries and increasing pillar spacing ($s = 5 \mu\text{m}, 10 \mu\text{m}, 20 \mu\text{m}, 40 \mu\text{m}$).

Spacing (μm)	Square ($5 \times 5 \mu\text{m}^2$)	Square ($10 \times 10 \mu\text{m}^2$)	Square ($20 \times 20 \mu\text{m}^2$)	Square ($40 \times 40 \mu\text{m}^2$)	Circular ($10 \times 10 \times \pi \mu\text{m}^2$)	Triangular ($0.5 \times 10 \times 10 \mu\text{m}^2$)	6-point Star ($10 \times 10 - 23.38 \mu\text{m}^2$)
5							
10							
20							
40							
80							
160							
320							

Figure 4: Optical microscope images of Al_2O_3 nanoparticle deposits after evaporation of 0.05 wt.% Al_2O_3 -ethanol droplets on square (with different size of the pillars from 5 to 40 μm), circular, triangular and star shaped pillars for different pillar spacings $s = 5, 10, 20, 40, 80, 160, 320 \mu\text{m}$. Scale bar is 1 mm.

5. DROPLETS MOTION ON STRIATED SURFACE AND TEMPERATURE GRADIENTS

Microscale droplet motion can be induced under the influence of surface tension gradients on the substrates. Firstly, droplet motion on substrates decorated with microstructures was studied. Droplets in the Cassie–Baxter state, straddling the boundary of two contrasting striated surfaces, move along the wettability contrast in order to reduce the overall surface free energy. The results show the importance of the average solid fraction and contrasting fraction in a wide range of given geometries across the boundary on droplet motion. A unified criterion for contrasting striated surfaces, which describes the displacement and the velocity of the droplets, is suggested, providing guidelines for droplet manipulation on micro-striated/railed surfaces, Figure 5. Secondly, droplet motion driven by thermocapillary force on slippery liquid infused porous surfaces (SLIPs) was studied. SLIPs exhibit low hysteresis and a thermal gradient of $\sim 1\text{K/mm}$ can drive the droplet to move. The influences of thermocapillary force and solutal Marangoni flow have been investigated for binary mixture droplets [3].

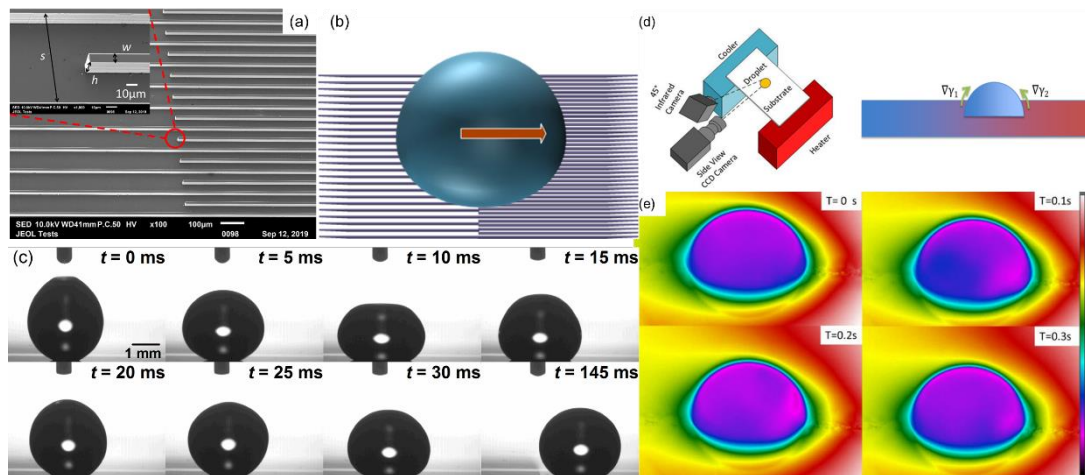


Figure 5: SEM images of the surface structure at a sharp contrasting boundary. (b) Schematic diagram showing how the droplet moves across the boundary. (c) Sequential photography of a $9\ \mu\text{l}$ droplet moving on the contrasting boundary. (d) Schematic diagram showing the experimental setup for thermocapillary motion. (e) Sequential photography of a droplet moving on the surface with thermal gradient.

REFERENCES

- [1] Y. Chen, A. Askounis, V. Koutsos, P. Valluri, Y. Takata, S. K. Wilson, and K. Sefiane, On the Effect of Substrate Viscoelasticity on the Evaporation Kinetics and Deposition Patterns of Nanosuspension Drops, *Langmuir* (2020) **36**, 1, 204–213
- [2] M. Efstratiou, J. Christy, K. Sefiane, Crystallization-Driven Flows within Evaporating Aqueous Saline Droplets, *Langmuir*, (2020) **36**, 18, 4995–5002
- [3] H. Zhao, D. Orejon, C.M. Dover, P. Valluri, M. Shanahan, K. Sefiane, Droplet motion on contrasting striated surfaces, *Applied Physics Letters*, (2020) **116**, 251604.